Journal of Applied Polymer Science

Thermal–Oxidative Degradation and Accelerated Aging Behavior of Polyamide 6/Epoxy Resin-Modified Montmorillonite Nanocomposites

Lei Xia, Jinsu Xiong, Baoqing Shentu, Zhixue Weng
State Key Lab of Chemical Engineering, Department of Chemical and biological Engineering, Zhejiang University, 38 Zheda Road, Hangzhou 310027, China
Correspondence to: B. Shentu (E-mail: shentu@zju.edu.cn)

ABSTRACT: Polyamide 6 (PA6) nanocomposites based on epoxy resin-modified montmorillonite (EP-MMT) were prepared by melt processing using a typical twin-screw extruder. X-ray diffraction combined with transmission electron microscopy was applied to elucidate the structure and morphology of PA6/EP-MMT nanocomposites, suggesting a nearly exfoliated structure in the nanocomposite with 2 wt % EP-MMT (PA6/2EP-MMT) and a partial exfoliated-partial intercalated structure in PA6/4 wt %EP-MMT nanocomposite (PA6/4EP-MMT). The thermogravimetric analysis under air atmosphere was conducted to characterize the thermal–oxidative degradation behavior of the material, and the result indicated that the presence of EP-MMT could inhibit the thermal-oxidative degradation of PA6 effectively. Accelerated heat aging in an air circulating oven at 150°C was applied to assess the thermal–oxidative stability of PA6 nanocomposites through investigation of reduced viscosity, tensile properties, and chemical structure at various time intervals. The results indicated that the incorporation of EP-MMT effectively enhanced the thermal–oxidative stability of PA6, resulting in the high retention of reduced viscosity and tensile strength, and the low ratio of terminal carboxyl group to amino group. © 2014 Wiley Periodicals, Inc. J. Appl. Polym. Sci. **2014**, *131*, 40825.

KEYWORDS: aging; clay; polyamide 6; thermogravimetric analysis (TGA)

Received 20 November 2013; accepted 4 April 2014
DOI: 10.1002/app.40825

INTRODUCTION

Polymer nanocomposites (PN) have been a hot topic for advanced scientific research and industrial development over the last decades, presenting a variety of applications in transportation, aerospace, construction, electrical devices, and food packaging.[1,2] Although many organic or inorganic nanomaterials can be incorporated for the modification of a polymer, layered silicates (clay) is considered to be an optimum choice because of its natural abundance, low product cost, high mechanical strength and chemical resistance, and intercalation properties from the view of modification efficiency.[3–5] Out of all of the methods to prepare polymer/clay nanocomposites, the approach based on direct melt intercalation is perhaps the most versatile and environmentally benign.[6]

Among kinds of clay, montmorillonite (MMT) is the most frequently employed. MMT belongs to the family of 2 : 1 layered silicates whose one layer contains one central octahedral sheet (of either aluminium hydroxide or magnesium hydroxide) condensed to two parallel tetrahedral sheets (of silica), via silica oxygen apices to octahedral hydroxyl planes.[7] The crystal structure of MMT is shown in Figure 1[8] Pristine MMT is hydrophilic and thus naturally incompatible with most polymers. For this reason, it is widely considered that organic treatment of MMT is the key issue for achieving a nanocomposites.[9] Generally, the compatibility of polymer and MMT can be improved via ion-exchange reactions with organic surfactants, including mainly quaternary alkylammonium cations in aqueous medium.[5,10,11] However, there are some limitations of this method, due to high water consumption, inefficiency single ion-exchange, high cost, limited number of available quaternary alkylammonium compounds, and their weak thermal stability.[12–14] Hence, some studies focused on the solid-state reaction based on the ion-dipole interaction.[15–19] In the ion-dipole interaction, organic molecules with polar groups are attached to the interlayer cations. The absence of solvents in proceeding the preparation is environmentally good and makes the process more suitable for industrialization.[20] Heretofore, a wide variety of compounds have been intercalated in MMT by ion-dipole interaction, such as amines,[16] aniline salts,[17] aldehydes,[12] alcohols,[12] imidazoles,[17] block copolymers,[19] epoxy resin,[15,21] etc.

Polyamide 6 (PA6) based MMT nanocomposites (PA6/MMT) were the first studied systems under investigation among PN, pioneered by Toyota research group.[22] Since then, extensive

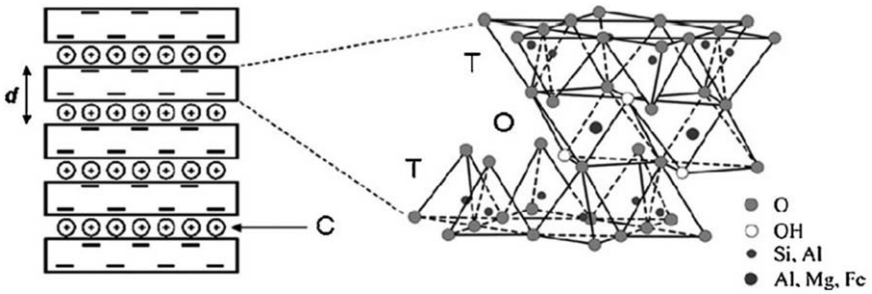

Figure 1. Crystal structure of MMT.

work has been devoted on various aspects of these materials.[10,11] Nevertheless, the thermal–oxidative degradation behavior and the long-term stability of PA6 nanocomposites have been insufficiently studied. These performances are not negligible in using the materials in practical products, since plastics experience irreversible structure changes as a result of their exposure to environmental elements, principally oxygen and heat.[5,23] It is well established that the thermal–oxidation of PA6 begins by abstraction a hydrogen atom from a N-vicinal methylene group and propagates by oxidation of the formed macroradical.[5,24] According to the sensitivity of PA6 to thermal–oxidative degradation, the addition of MMT particles in nanometer scale has significant influence on thermal characteristics of the PA6 matrix. The effect of MMT nano-filler on the thermal-oxidative degradation pathway of PA6 is rather complicated, since silicates constitute barriers to the diffusion of oxygen and the volatile degradation products but they also provoke the decomposition of the polymer matrix caused through initiating sites on the MMT or through releasing water.[5,8,25–27] It was also suggested that only exfoliated PN exhibited improved thermal–oxidative stability and that agglomerated MMT particles did not show similar effect.[25,28]

Currently, much of the research on the thermo-oxidative degradation of polymer/clay nanocomposites have focused on analyzing the gaseous decomposition products evolved during the degradation process, using hyphenated techniques such as thermogravimetric analysis (TGA) combined with mass spectrometry (MS) and Fourier transform infrared spectroscopy (FT-IR), as well as pyrolysis-gas chromatography combined with MS.[25,29,30] However, they were not able to provide direct information on the chemical changes undergone by the nanocomposites upon thermal–oxidative degradation, leading to contradictory and sometimes erroneous conclusions.[30,31] Alternatively, accelerated aging tests were used by some researchers. In this way, changes in bulk properties like molecular weight, mechanical performance, yellowing, and crystallization behavior can be recorded at ordinary time interval of exposure.[4,5,32–34] Ito et al.[32] have measured the changes in bulk properties of pure PA6 and PA6/MMT nanocomposites under thermal–oxidative aging test at various temperatures and found that the performance reduction rate of nanocomposite was faster than that of pure PA6, since the tetraalkylammonium that applied as a surface active agent affected the degradation reaction. Kiliaris et al.[5] have studied the long-term thermal-oxidative aging behavior of PA6 nanocomposites based on stearylbenzyldimethyl-ammonium chloride modified bentonite and proposed that the clay filler restricted degradation, thus prolonging service life. However, as far as we know, there has no literature about the effect of organic MMT modified through solid-state reaction to the thermal–oxidative aging behavior of PA6.

In this work, PA6 nanocomposites based on epoxy resin-modified montmorillonite (PA6/EP-MMT) were prepared by melt processing using a typical twin-screw extruder. Accelerated heat aging in an air circulating oven at 150°C was applied to assess the thermal–oxidative stability of PA6 nanocomposites through investigation of reduced viscosity, tensile properties, and chemical structure at various time intervals. TGA in air was also conducted to characterize the thermal–oxidative degradation behavior of the material. On the basis of these results, we made an attempt to gain a better understanding of the influence of EP-MMT on the thermal–oxidative aging behavior of PA6.

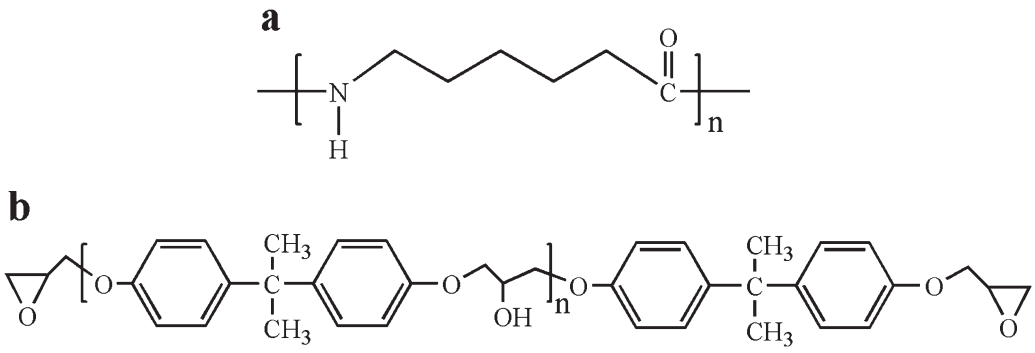

Figure 2. Chemical structure formulas of (**a**) PA6, and (**b**) epoxy resin.

EXPERIMENTAL

Materials

PA6 (1013B) used in this study was obtained from Ube Kosan Co., Ltd. (Japan), with a relative viscosity of 2.7. Figure 2(a) shows the repeat unit of PA6. EP-MMT, which was the sodium montmorillonite modified by solid-state reaction with epoxy compound, with organic content of 28.5 wt %, was kindly supplied by Hangzhou Hongyan Electrical Co., Ltd. (Zhejiang, China). The chemical structure formula of the surfactant epoxy resin is shown in Figure 2(b).

Specimen Preparation

Before processing, the PA6 and EP-MMT were carefully dried for 12 h at 100°C in a vacuum oven. PA6/EP-MMT nanocomposites with 2 and 4 wt % EP-MMT (abbreviated as PA6/2PMMT and PA6/4PMMT, respectively) were prepared via a melt-compounding method using a twin-screw extruder (HAAKE Polylab OS, Thermo Electron Erlangen GmbH, Germany) having L/D ratio of 40 : 1. The screw speed was maintained at 200 rpm and the temperature profiles were between 230°C and 245°C. The obtained extrudates were pelletized and dried at 80°C *in vacuo* for 12 h. Then, some of the granules were used for the chemical analysis, and some of them were injected into a standard dumbbell specimen with an injection moulding machine (HAAKE MiniJet II, Thermo Electron Erlangen GmbH, Germany) for the mechanical property measurements. In addition, the pure PA6 was also prepared by the same process for comparison.

Thermal–Oxidative Aging

The obtained dumbbell-shaped specimens and granular samples of PA6 and PA6 nanocomposites samples were subjected to thermal–oxidative aging in an air circulating oven at 150°C ± 1°C, respectively. The samples were taken out at regular time intervals and used for mechanical and chemical characterization.

Measurement

X-ray Diffraction. In order to probe the structure of the prepared nanocomposite, X-ray diffraction (XRD) studies were performed on an X-ray power diffractometer using Cu$K\alpha$ radiation ($\lambda = 0.15406$ nm) (XRD-6000, Shimadzu Co., Japan) operated under a voltage of 35 kV and a current of 100 mA. Corresponding data were collected from 3° to 10° at a scanning rate of 1°/min.

Transmission Electron Microscopy. To study the dispersion of EP-MMT layers in the polymer matrix, transmission electron micrographs (TEM) were performed on a JEOL JEM-1230 apparatus (JEOL Co., Japan) at an accelerating voltage of 120 kV. Each composite sample with a thickness of 80 nm was prepared using an ultra cryo-microtome cutting apparatus at −130°C.

Thermogravimetric Analysis. The TGA measurements were performed under air atmosphere with a Pyris 1 thermogravimetric analyzer (Perkin-Elmer, Inc.) to study the thermal–oxidative degradation of PA6 nanocomposites. Samples (2 ± 0.2 mg) were heated from room temperature to 700°C at a heating rate of 20°C/min under a gas flow rate of 30 mL/min. The temperature reproducibility of TGA is ±1°C and the error range of the mass is ±0.6%.

Reduced Viscosity. A sample of about 0.5 g was dissolved in 100 mL of formic acid. The mixture was high speed centrifuged to remove the MMTs, and then filtrated by a sand core funnel. The time of outflow of the solution was measured with an Ubbelohde viscometer in a water bath at 25°C according to ISO 307–1984. Then, the reduced viscosity (η) was calculated with the following equation:

$$\eta = \left(\frac{t}{t_0} - 1\right) \times \frac{1}{C} \tag{1}$$

where t is the outflow time of the PA6 solution (s), t_0 is the outflow time of the solvent (s), and C is the concentration of the PA6 solution (g/mL).

Tensile Properties. Tensile tests were carried out according to the ISO 527/1–1993 standards at 23°C using dumbbell-shaped specimens with dimension of 75 × 4 × 2 mm. The tests were performed using a tensile machine (Zwick/Roell Z202, Zwick/Roell Group, Germany) at a crosshead speed of 10 mm/min. At least five specimens were used for each sample.

End Group of PA6[33,34]. ***The terminal carboxyl group.*** A sample of about 0.3 g was dissolved in 20 mL of phenylcarbinol at 150°C. Then, 3 mL of propyl alcohol was added, and the hot solution was titrated by NaOH (ca., 0.02 mol/L), with phenolphthalein used as an indicator. The concentration of carboxylic acid (X) was calculated according to the following equation:

$$X = \frac{(a-b)n}{w} \times 10^{-3} \tag{2}$$

where a is the consumption volume of the NaOH solution for the sample of PA6 (mL), b is the consumption volume of the NaOH solution for the solvent (mL), n is the molar concentration of the NaOH solution (mol/L), and w is the weight of the sample (g).

The terminal amino group. A sample of about 0.3 g was dissolved in 25 mL of a mixing solution of phenol and methyl alcohol (volume ratio 1 : 1) at 55°C. The solution, after that, was titrated with HCl (ca., 0.005 mol/L) with thymol blue as the indicator. The concentration of the end amine groups (Y) was calculated according to the following equation:

$$Y = \frac{(A-B)m}{W} \times 10^{-3} \tag{3}$$

where A is the consumption volume of the HCl solution (mL) for the sample of PA6, B is the consumption volume of the HCl solution for the solvent (mL), m is the molar concentration of the HCl solution (mol/L), and W is the weight of the sample (g).

RESULTS AND DISCUSSION

Structural Characterization of PA6/EP-MMT Nanocomposites

XRD and TEM are complementary techniques which can be used to elucidate the structure and morphology of PN. XRD gives quantitative information about the internal structure while TEM offers a qualitative understanding of the dispersion status

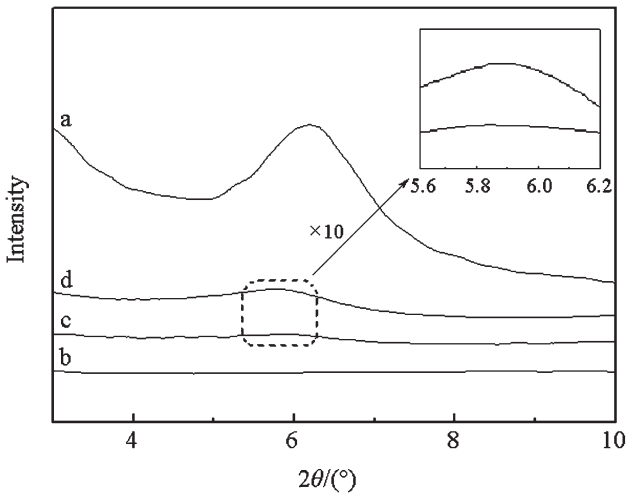

Figure 3. XRD patterns of (**a**) EP-MMT, (**b**) pure PA6, (**c**) PA6/2EP-MMT, (**d**) PA6/4EP-MMT (Inset: the 10-fold enlarged patterns of c and d at $2\theta = 5.6°–6.2°$).

of the nano-materials in the polymer matrix through direct visualization.[30,35]

Figure 3 displays the XRD patterns of EP-MMT and PA6/EP-MMT nanocomposites. The pattern of EP-MMT showed a prominent basal reflection at $2\theta = 6.18°$ that corresponding to a *d*-spacing of 1.49 nm, according to Bragg's law. On the other hand, this basal reflection peak was hardly observed in the diffractogram of PA6/2EP-MMT, suggestive of extensive layer separation and formation of a nearly exfoliated structure. For PA6/4EP-MMT nanocomposites, a weak shoulder at around $2\theta = 5.78°$ (*d*-spacing = 1.59 nm) was observed in Figure 3(d), implying an intercalated structure via melt extrusion processing and the presence of a partially intercalated/partially exfoliated structure in PA6/4EP-MMT.[36]

TEM images of PA6/EP-MMT nanocomposites are shown in Figure 4, where the dark lines represented MMT platelets while the gray/white background corresponded to the PA6 matrix. These images supported the interpretation of the X-ray results. It was observed in Figure 4(a) that individual silicate layers were well-dispersed in the polymer matrix. Whereas, some multilayer orders were visible in Figure 4(b), indicating the existence of both exfoliated and intercalated structures.

Thermal–Oxidative Degradation of PA6/EP-MMT Nanocomposites

The thermal–oxidative degradation of pure PA6 and PA6/EP-MMT nanocomposites was investigated by a thermogravimetic analyzer under air atmosphere at a heating rate of 20°C/min. The result TG curves are shown in Figure 5. A distinct two-step degradation process was observed for all samples. The main weight loss occurred in the first step (from 400°C to 500°C).

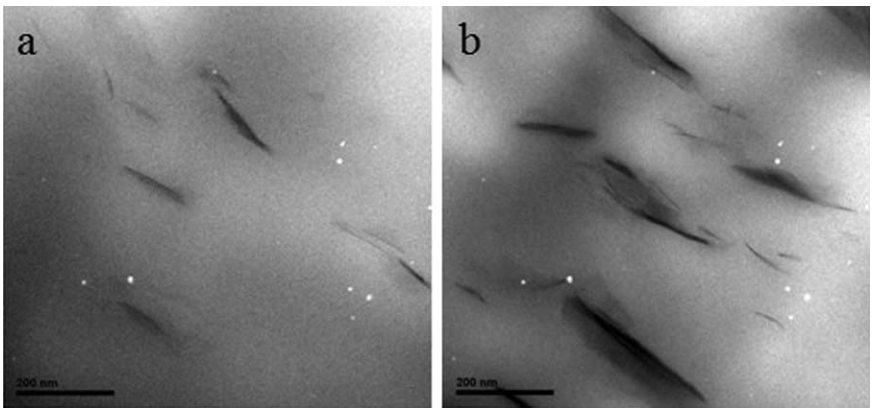

Figure 4. TEM images of (**a**) PA6/2EP-MMT, (**b**) PA6/4EP-MMT.

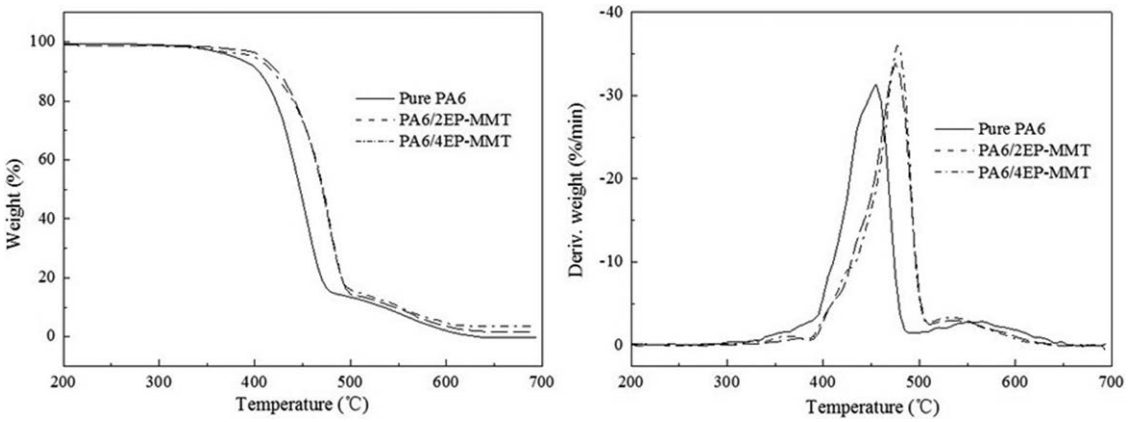

Figure 5. TG and DTG curves of pure PA6 and PA6/EP-MMT nanocomposites in air.

Table I. Results of TGA in Air of Pure PA6 and PA6/EP-MMT Nanocomposites

Sample	$T_{5\%}$ (°C)	$T_{50\%}$ (°C)	T_{max} (°C)	Char residue (%)
Pure PA6	378	447	455	0
PA6/2EP-MMT	407	471	475	1.6
PA6/4EP-MMT	399	472	476	3.5

The second slow weight loss may be ascribed to the char oxidation due to the existence of oxygen at high temperature.[37] From the TG curves, the temperature at which 5 wt % degradation occurred ($T_{5\%}$), the temperature at which 50 wt % degradation occurred ($T_{50\%}$), the temperature at which the maximum degradation rate occurred (T_{max}), and the char residue at the end of degradation for the samples are summarized in Table I.

According to previous reports, the effects of EP-MMT on the thermal–oxidative degradation of PA6 can be classified into three kinds: (1) organic surfactant with lower thermal–oxidative stability will decompose earlier than PA6, and the decomposition products may accelerate the degradation of PA6 chains; (2) the interface interaction between EP-MMT and PA6 chains results in restriction of segmental mobility, thus improves thermal–oxidative stability;[38,39] (3) the barrier effect of EP-MMT is able to slow down the volatilization of thermal–oxidative degradation products from inner matrix into external environment, as well as the transportation of the heat and oxygen from surface to inner matrix, thus weakens the thermal–oxidative degradation rate;[27,40] (4) the reactive functional groups in the EP-MMT filler may act as scavenger of intermediate peroxyradicals, thus partially inhibit the thermal–oxidative degradation of PA6.[5,41] As seen from Figure 5 and Table I, PA6/EP-MMT nanocomposites showed obviously higher characteristic temperatures than those of pure PA6, indicating that the presence of EP-MMT effectively restrained the thermal–oxidative degradation of PA6. That was to say, the stabilization effect of EP-MMT was dominant during thermal–oxidative degradation of PA6/EP-MMT nanocomposites, resulting to the improved thermal–oxidative stability.

Furthermore, it was visualized that the $T_{5\%}$ of PA6/2EP-MMT was 8°C higher than that of PA6/4EP-MMT, while the $T_{50\%}$ and the T_{max} were almost the same. It was speculated that PA6/2EP-MMT with exfoliated structure presented better thermal–oxidative stability than PA6/4EP-MMT during the early degradation stage, and became similar afterward. The TG curve of EP-MMT under air atmosphere at a heating rate of 20°C/min was displayed in Figure 6. The $T_{5\%}$ of EP-MMT was 336°C, which was much higher than most quaternary alkylammonium compounds while still lower than that of PA6.[27] The decomposition products of EP-MMT may catalyze the breakage of PA6 chains, thus accelerate thermal–oxidative degradation. This may be one reason why PA6/2EP-MMT presented better thermal–oxidative stability than PA6/4EP-MMT during the early degradation stage. The other reason could be related to the dispersion status of EP-MMT in the PA6 matrix, suggesting better stabilizing effect obtained due to exfoliated structure.

Reduced Viscosity of PA6/EP-MMT Nanocomposites

Throughout oven aging, changes in molecular weight are detected as a result of PA6 thermal–oxidative degradation. It is essential in understanding the physical properties of polymer by gaining knowledge on the molecular weight.[5] It is well known that the reduced viscosity which is equal to the ratio of the relative viscosity increment to the mass concentration of the polymer characterizes the viscosity average molecular weight of polymers.[42] Therefore, the variation of the reduced viscosity of pure PA6 and PA6/EP-MMT nanocomposites with the aging time at 150°C was investigated, which is shown in Figure 7.

The reduced viscosity of pure PA6 before processing was 162.3 mL/g, but that of pure PA6 after melt extruding was 154.6 mL/g. The reduction of the reduced viscosity may be resulted from the molecular thermal–mechanical degradation led by the high processing temperature and sheer force of the twin-screw during melt extruding.[33] On the other hand, the reduced viscosity of PA6/2EP-MMT and PA6/4EP-MMT after melt extruding was 152.2 and 148.3 mL/g, respectively, even lower than that of PA6. The similar phenomenon was also reported in other literatures.[30,43] It can be concluded that the nanocomposites specimens suffered more severe degradation upon preparation, and the more nanofiller added, the more reduction of molecular weight occurred. This may be related to the decomposition of EP-MMT during melt processing, the decomposition products may catalyze the breakage of PA6 chains, thus decreased the reduced viscosity of PA6/EP-MMT nanocomposites.

It can be visualized from Figure 7 that the reduced viscosity of all samples showed a marginal increase at the early stage of thermal–oxidative aging. Subsequently, it decreased gradually and became to form a clear plateau at last. The presented trend of increasing followed with declining was also observed by Yang et al.[33,34] and Zhao et al.[44] According to Yang et al.'s report, it was explained that the molecular crosslinking reaction of PA6 predominated during the primary aging time, leading to the increase of the reduced viscosity, while the molecular degradation of the polymer predominated afterward, resulting in the decrease of the reduced viscosity.

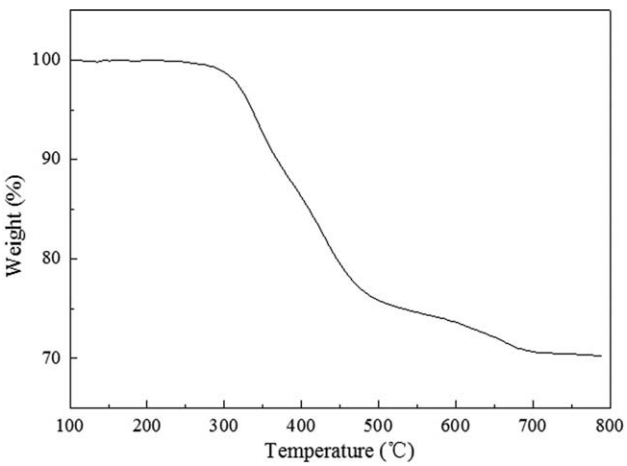

Figure 6. TG curve of EP-MMT.

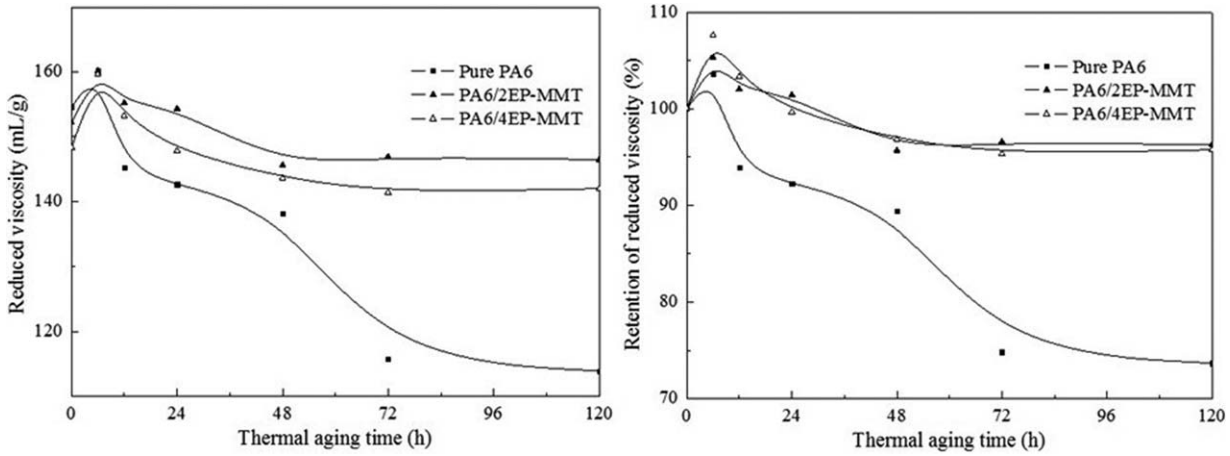

Figure 7. Reduced viscosity of pure PA6 and PA6/EP-MMT nanocomposites as a function of aging time.

For pure PA6, the reduced viscosity rose during the first 6 h and then it declined drastically and reached 74% in 120 h. By contrast, the reduced viscosity of PA6/EP-MMT nanocomposites declined more moderately, and had a higher retention during the aging procedure. The result which was different to Ito et al.'s conclusion[32] indicated that the addition of EP-MMT could restrict the molecular degradation of PA6 effectively, thus enhanced the long-term thermal–oxidative ability. The stabilization should attribute to the barrier effect of well-dispersed EP-MMT in the PA6 matrix that retarded the diffusion of heat, oxygen, and volatile degradation products, which was widely accepted by researchers.[25,30] However, higher content of EP-MMT in the PA6 matrix led to a decrease of stabilizing effect due to worse dispersion and more decomposed organic surfactant, resulting in the similar reduced viscosity retention of PA6/4EP-MMT compared with that of PA6/2EP-MMT.

Mechanical Performance of PA6/EP-MMT Nanocomposites

The mechanical properties will also change when a polymer suffers thermal–oxidative degradation in addition to the molecular weight. Hence, the tensile properties are used to measure the degree of polymer degradation here. The tensile strength and elongation at break of pure PA6 and PA6/EP-MMT nanocomposites aging with time at 150°C were determined, and the results are shown in Figures 6 and 7.

In lots of literatures, the mechanical strength of PA6 was greatly improved by the compounding and the dispersion of the organic modified MMT.[10,11] In this article, as shown in Figure 8, the tensile strength of PA6, PA6/2EP-MMT and PA6/4EP-MMT were 62.5, 69.2, and 72.6 MPa, respectively. The tensile strength of all the samples presented a similar trend to the reduced viscosity, beginning with increase and decreasing afterward. The change of tensile strength should be ascribed to the dominated molecular crosslinking reaction at the beginning of aging and the dominated molecular degradation afterward, as well as to post-crystallization of amorphous phase and cleaved chains.[44,45] As shown in Figure 8, the decrease rate of the tensile strength of PA6/EP-MMT nanosomposites was slower than that of the pure PA6 during the whole aging procedure, suggestive of the stabilizing effect of EP-MMT. In addition, the tensile strength of PA6/2EP-MMT continued to increase with aging time during the first 12 h, while the other two samples began to lost stiffness after 6 h.

The service life of a polymer in a specific environment is usually reflected by the time required for a 50% reduction in the value of an important property, such as elongation at break.[5,46]

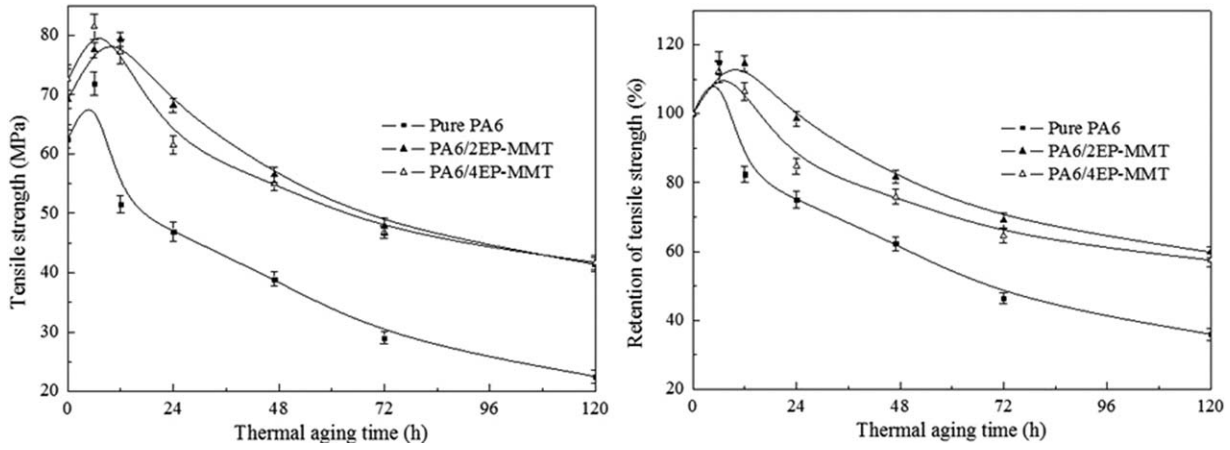

Figure 8. Tensile strength of pure PA6 and PA6/EP-MMT nanocomposites as a function of aging time.

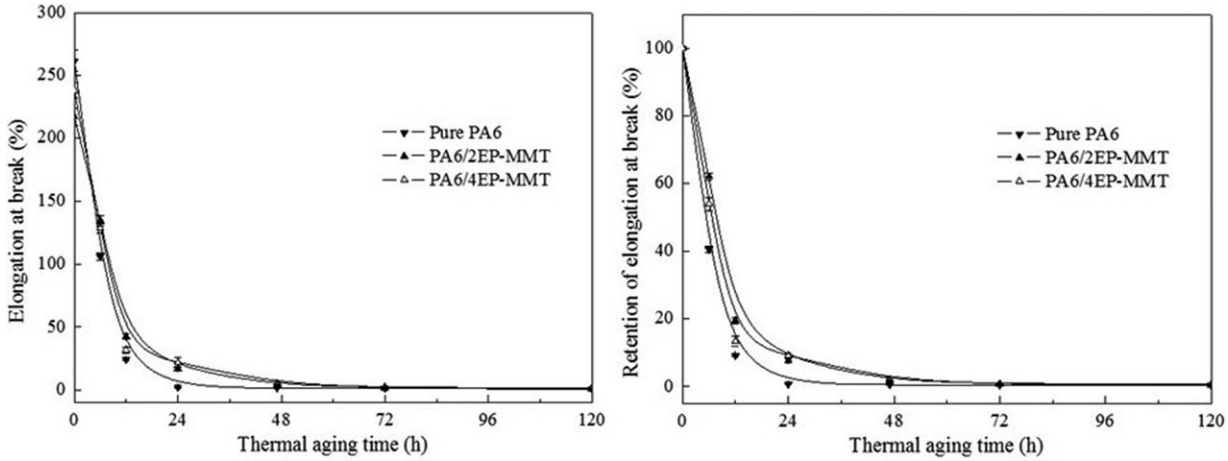

Figure 9. Elongation at break of pure PA6 and PA6/EP-MMT nanocomposites as a function of aging time.

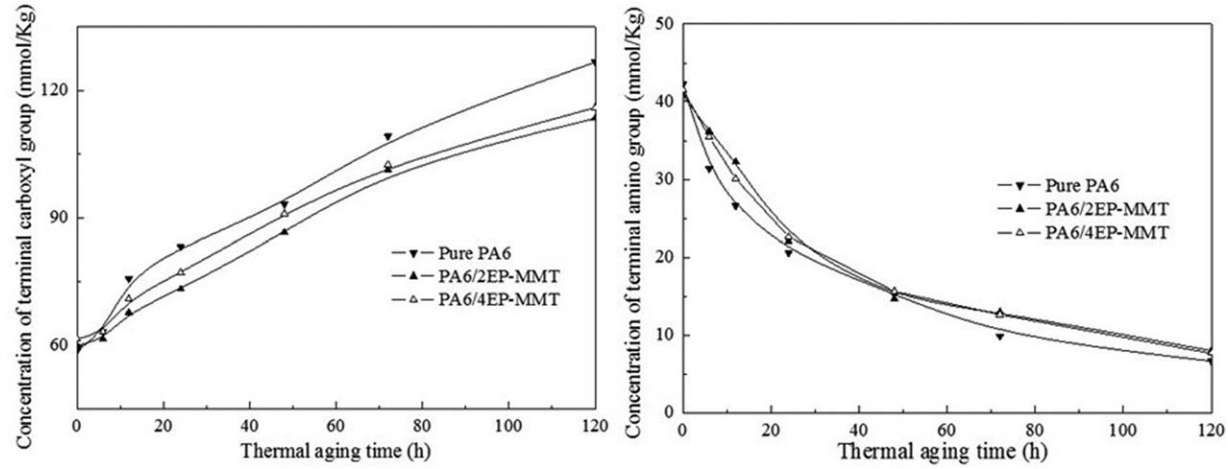

Figure 10. Concentration of terminal carboxyl and amino group of pure PA6 and PA6/EP-MMT nanocomposites as a function of aging time.

Turning on Figure 9, the elongation at break of materials all decreased rapidly to a plateau with increasing aging time. It was found that the level of a 50% reduction was accomplished after 6 h in the case of the pure PA6. This reduction was delayed in the presence of EP-MMT, prolonging service life. The result again indicated that the incorporation of EP-MMT into the PA6 matrix was helpful to enhance the thermal–oxidative stability.

Chemical Structure of PA6/EP-MMT Nanocomposites

It is well known that the rate of thermal–oxidation of polyamides depends mostly on the content and ratio of the terminal carboxyl and amino groups.[47,48] The thermal–oxidative degradation of PA6 would be promoted by carboxylic acid formed during aging, while the terminal amino group has a thermal–oxidative stabilization effect on PA6.

The chemical structure (terminal carboxyl group and terminal amino group) of PA6 samples during aging at 150°C is shown in Figure 10, while the ratio of terminal carboxyl to amino group is shown in Figure 11. With increase of aging time, the terminal carboxyl group concentration rose and the terminal amino group concentration fell monotonously for PA6. The rupture of the amido-bond and the adjacent C—C bond resulted in the formation of the carboxylic acid, carbonyl, and the terminal amino group. The decline of the concentration of

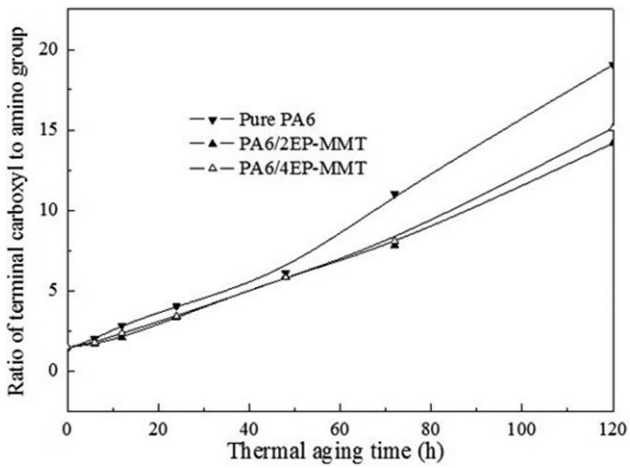

Figure 11. Ratio of terminal carboxyl to amino group of pure PA6 and PA6/EP-MMT nanocomposites as a function of aging time.

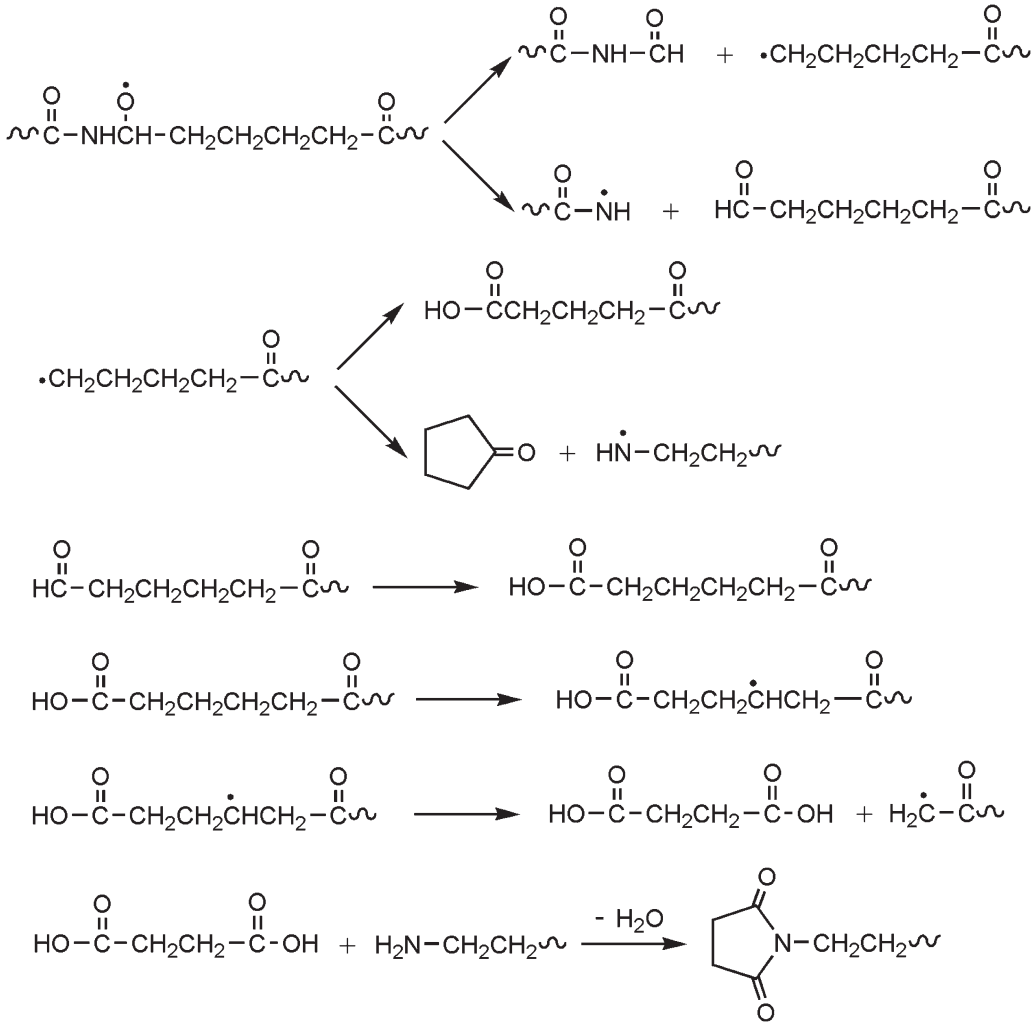

Figure 12. The schematic description of the reactions leading to the change of carboxylic and amino end-groups.

the terminal amino group of PA6 perhaps resulted from the reaction between end amine groups and carboxylic acids, or producing the compounds such as tertiary amine, or producing the compounds escaped from the matrix by aging degradation.[34,44] Figure 12 was the schematic description of the reactions.[34,49]

Before aging, the terminal carboxyl group concentration of pure PA6 was lower than that of PA6/EP-MMT nanocomposites, while the terminal amino group concentration was higher, due to the more severe degradation of PA6/EP-MMT nanocomposites suffered during melt blending process.[43] However, during aging, the terminal carboxyl group concentration of pure PA6 became higher than that of PA6/EP-MMT nanocomposites, while the terminal amino group concentration became relatively lower, especially in comparison with PA6/2EP-MMT. The change of the ratio of terminal carboxyl to amino group appeared a similar trend. The result definitely indicated that the introduction of EP-MMT was favorable to the thermal–oxidative stability of PA6.

CONCLUSION

EP-MMT prepared through solid-state reaction was introduced to the PA6 matrix by melt processing using a typical twin-screw extruder. XRD combined with TEM was used to elucidate the structure and morphology of PA6/EP-MMT nanocomposites, suggestive of an exfoliated structure in PA6/2EP-MMT and an exfoliated-intercalated structure in PA6/4EP-MMT. TGA result under air atmosphere indicated that the stabilization effect of EP-MMT was dominant during thermal–oxidative degradation of PA6/EP-MMT nanocomposites, resulting to the improved thermal–oxidative stability. More specifically, PA6/2EP-MMT with exfoliated structure presented better thermal–oxidative stability than PA6/4EP-MMT during the early degradation stage, and became similar afterward. PA6/EP-nanocomposites were subjected to accelerated aging at 150°C to estimate its long-term thermo-oxidative stability compared with the virgin material. Changes in reduced viscosity, tensile properties, and chemical structure were monitored at various time intervals. The results indicated that PA6/EP-MMT nanocomposites maintained

higher retention of reduced viscosity and tensile strength, and lower ratio of terminal carboxyl group to amino group than the pure PA6. Furthermore, PA6/2EP-MMT and PA6/4EP-MMT showed similar thermal–oxidative aging stability, since higher content of EP-MMT in the PA6 matrix caused worse dispersion and more decomposed organic surfactant thus weakened stabilization effect.

REFERENCES

1. Camargo, P. H. C.; Satyanarayana, K. G.; Wypych, F. *Mater. Res.* **2009**, *12*, 1.
2. Jeon, I. Y.; Baek, J. B. *Materials* **2010**, *3*, 3654.
3. Alexandre M.; Dubois, P. *Mater. Sci. Eng., R* **2000**, *28*, 1.
4. Choudhury, A.; Bhowmick, A. K.; Soddemann, M. *Polym. Degrad. Stabil.* **2010**, *95*, 2555.
5. Kiliaris, P.; Papaspyrides, C.D.; Pfaendner, R. *Polym. Degrad. Stabil.* **2009**, *94*, 389.
6. Liu, X. H.; Wu, Q. J.; Berglund, L. A.; Lindberg, H.; Fan, J. Q.; Qi, Z. N. *J. Appl. Polym. Sci.* **2003**, *88*, 953.
7. Kumara, A. P.; Depana, D.; Tomerb, N. S.; Singh, R. P. *Prog. Polym. Sci.* **2009**, *34*, 479.
8. Chrissafis, K.; Bikiaris, D. *Thermochim. Acta* **2011**, *523*, 1.
9. Li, Y.; Guo, Z. X.; Yu, J. *Macromol. Mater. Eng.* **2005**, *290*, 649.
10. Ray, S. S.; Okamoto, M. *Prog. Polym. Sci.* **2003**, *28*, 1539.
11. LeBaron, P. C.; Wang, Z.; Pinnavaia, T. J. *Appl. Clay Sci.* **1999**, *15*, 11.
12. Beall, G. W.; Goss, M. *Appl. Clay Sci.* **2004**, *27*, 179.
13. Gao, Z.; Liu, K.; Pan, W. P.; Vaia, R.; Hunter, D.; Singh, A. *Thermochim. Acta* **2001**, *367*, 339.
14. Xie, W.; Xie, R.; Pan, W. P.; Hunter, D.; Koene, B.; Tan, L. S.; Vaia, R. *Chem. Mater.* **2002**, *14*, 4837.
15. Ishida, H.; Campbell, S.; Blackwell, J. *Chem. Mater.* **2000**, *12*, 1260.
16. Merinska, D.; Malac, Z.; Pospisil, M.; Weiss, Z.; Chmielova, M.; Capkova, P.; Simonik, J. *Comp. Interf.* **2002**, *9*, 529.
17. Yoshimoto, S.; Osashi, F.; Kameyama, T. *Solid State Commun.* **2005**, *136*, 251.
18. Awad, W. H.; Gilman, J. W.; Nyden, M.; Harris Jr., R. H.; Sutto, T. E.; Callahan, J.; Truvole, P. C.; DeLong, H. C.; Fox, D. M. *Thermochim. Acta* **2004**, *409*, 3.
19. Zha, W. B.; Han, C. D.; Han, S. H.; Lee, D. H.; Kim, J. K.; Guo, M. M.; Rinaldi, P. L. *Polymer* **2009**, *50*, 2411.
20. Paiva, L. B.; Morales, A. R.; Valenzuela-Díaz, F. R. *Appl. Clay Sci.* **2008**, *42*, 8.
21. Eissa, M. M.; Youssef, M. S. A.; Ramadan, A. M.; Amin, A. *Polym. Eng. Sci.* **2013**, *53*, 1011.
22. Okada, A.; Kawasumi, M.; Kurauchi, T. *Polym. Prepr. (Am. Chem. Soc., Div. Polym. Chem.)* **1987**, *28*, 447.
23. Ito, M.; Nagai, K. *J. Appl. Polym. Sci.* **2010**, *118*, 928.
24. Levchik, S. V.; Weil, E. D.; Lewin, M. *Polym. Int.* **1999**, *48*, 532.
25. Pramoda, K. P.; Liu, T. X.; Liu, Z. L.; He, C. B.; Su, H. *J. Polym. Degrad. Stabil.* **2003**, *81*, 47.
26. Zong, R. W.; Hu, Y.; Liu, N.; Li, S.; Liao, G. X. *J. Appl. Polym. Sci.* **2007**, *104*, 2297.
27. Bikiaris, D. *Thermochim. Acta* **2011**, *523*, 25.
28. Li, T. C.; Ma, J. H.; Wang, M.; Tjiu, W. C.; Liu, T. X.; Huang, W. *J. Appl. Polym. Sci.* **2007**, *103*, 1191.
29. Jang, B. N.; Wilkie, C. A. *Polymer* **2005**, *46*, 3264.
30. Zhang, X. G.; Loo, L. S. *Polymer* **2009**, *50*, 2643.
31. Zanetti, M.; Bracco, P.; Costa, L. *Polym. Degrad. Stabil.* **2004**, *85*, 657.
32. Ito, M.; Nagai, K. *J. Appl. Polym. Sci.* **2008**, *108*, 3487.
33. Yang, T.; Ye, L.; Shu, Y. *J. Appl. Polym. Sci.* **2008**, *110*, 856.
34. Shu, Y.; Ye, L.; Yang, T. *J. Appl. Polym. Sci.* **2008**, *110*, 945.
35. Morgan, A. B.; Gilman, J. W. *J. Appl. Polym. Sci.* **2003**, *87*, 1329.
36. Hu, Y.; Wang, S. F.; Ling, Z. H.; Zhuang, Y. L.; Chen, Z. Y.; Fan, W. C. *Macromol. Mater. Eng.* **2003**, *288*, 272.
37. Xia, L.; Li, F.; Shentu, B. Q.; Weng, Z. X. *J. Macromol. Sci. Phys.* **2013**, *52*, 310.
38. Rusu, G.; Rusu, E. *High Perform. Polym.* **2006**, *18*, 355.
39. Gilman, J. W. *Appl. Clay Sci.* **1999**, *15*, 31.
40. Yuan, X. P.; Li, C. C.; Guan, G. H.; Xiao, Y. N.; Zhang, D. *Polym. Degrad. Stabil.* **2008**, *93*, 466.
41. Allen, N. S.; Edge, M.; Corrales, T.; Childs, A.; Liauw, C. M.; Catalina, F.; Peinado, C.; Minihan, A.; Aldcroft, D. *Polym. Degrad. Stabil.* **1998**, *61*, 183.
42. Hu, M. J. Polymer Physics, Chapter 4; Fudan Industry Press: Shanghai, China, **2002**.
43. Davis, R. D.; Gilman, J. W.; VanderHart, D. L. *Polym. Degrad. Stabil.* **2003**, *79*, 111.
44. Zhao, X. W.; Li, X. H.; Ye, L.; Li, G. X. *J. Appl. Polym. Sci.* **2013**, *129*, 1193.
45. Cerruti, P.; Carfagna, C. *Polym. Degrad. Stabil.* **2010**, *95*, 2405.
46. Eriksson, P. A.; Boydell, P.; Eriksson, K.; Manson, J. A.; Albertsson, A. C. *J. Appl. Polym. Sci.* **1997**, *65*, 1619.
47. Lánská, B.; Šebenda, J. *Eur. Polym. J.* **1986**, *22*, 199.
48. Lánská, B.; Doskočilová, D.; Matisová-Rychlá, L.; Puffr, R.; Rychlý, J. *Polym. Degrad. Stabil.* **1999**, *63*, 469.
49. Li, R. F.; Hu, X. Z. *Acta Polym. Sin.* **2000**, *2*, 136.